

Silver segregation to θ' (Al₂Cu)-Al interfaces in Al-Cu-Ag alloysJulian M. Rosalie^aLaure Bourgeois^{b,c,d}^aStructural Materials Unit, National Institute for Materials Science, Tsukuba, 305-0047, Japan.^bMonash Centre for Electron Microscopy, Monash University, 3800, Victoria, Australia.^cARC Centre of Excellence for Design in Light Metals, Australia.^dDepartment of Materials Engineering, Monash University, 3800, Victoria, Australia.**Abstract**

θ' (Al₂Cu) precipitates in Al-Cu-Ag alloys were examined using high angle annular dark field scanning transmission electron microscopy (HAADF-STEM). The precipitates nucleated on dislocation loops on which assemblies of γ' (AlAg₂) precipitates were present. These dislocation loops were enriched in silver prior to θ' precipitation. Coherent, planar interfaces between the aluminium matrix and θ' precipitates were decorated by a layer of silver of two atomic layers in thickness. It is proposed that this layer lowers the chemical component of the Al- θ' interfacial energy. The lateral growth of the θ' precipitates was accompanied by the extension of this silver bi-layer, resulting in the loss of silver from neighbouring γ' precipitates and contributing to the deterioration of the γ' precipitate assemblies.

Keywords Aluminium alloys, Precipitation, Interfaces, Segregation**1 Introduction**

Aluminium-copper (Al-Cu) alloys are one of the most-studied precipitation strengthened alloy systems, in part due to their historic connection to the first precipitation-hardened Al alloys (Al-Cu-Mg) [1, 2]. Although Al-Cu alloys are amongst the earliest examples of precipitation-strengthened Al systems, alloys derived from these compositions, such as alloy designations 2014 and 2024, are still used in aerospace applications [3].

Al-Cu alloys derive a significant measure of their strength from the controlled precipitation of the θ' phase on the {100} planes of the Al matrix. These precipitates impede dislocation glide, enhancing the resistance to plastic deformation and hence increasing the yield strength. The Al-Cu system is also of great practical interest since the precipitation of the θ' phase can be manipulated through deformation and by the presence of various solutes, some of which (such as In, Sn and Cd) are potent even at trace levels [4, 5, 6].

Industrial variants of these alloys have considerably more complex compositions than simple, “model” alloys. Compositions are frequently chosen so as to improve mechanical properties through the formation of multiple precipitate phases. In Al-Cu-Mg alloys, for example, laths of S phase (Al₂CuMg) can form in addition to θ' plates. Multiple phase precipitation and the presence of additional elements in solution pose severe difficulties in clarifying the effect of any given element on θ' precipitation. Consequently, despite research spanning the past half-century, the mechanism(s) by which solute elements affect the precipitation of the θ' phase remain poorly understood.

The precipitate-matrix interface plays an important role in precipitation strengthening. A well-known example of this involves additions of Ag to Al-Cu-Mg alloys, which results in the precipitation of a phase termed Ω rather than θ' . Although the Ω phase shares the same bulk composition as θ' , it

forms with $\{111\}$ habit instead of $\{100\}$ and displays remarkable coarsening resistance. Drift corrected energy dispersive x-ray analysis [7] and 3D atom probe studies [8] have shown that Ag and Mg both segregate to the Ω -Al matrix interface. The Ω phase has a distinctive interface structure, with a bilayer of Ag atoms at the coherent interface with the matrix [9]. Density functional theory calculations indicated while substitution of either Mg or Ag alone was energetically unfavourable, a combination of both elements provided a lower-energy interface [10].

Recent work has shown that compositional changes at the θ' -matrix interface occur in other alloys. Silicon was found to segregate to the coherent $\{100\}$ interfaces of the θ' phase in Al-Cu-Si alloys, substituting for Cu sites in the precipitate [11]. It has also been demonstrated that the interface composition and structure of θ' in binary Al-Cu differs substantially from the bulk structure, with additional Cu atoms occupying octahedral interstices in the precipitate [12]. Despite these studies a detailed understanding of precipitate-matrix interfaces has yet to be developed in the majority of Al alloys.

Aluminium-copper-silver (Al-Cu-Ag) alloys are ideal for studying the effect of a third element on the precipitation of the θ' phase. Unlike many ternary systems (e.g. Al-Cu-Mg) the Al-rich region of the phase field contains only binary phases [13], eliminating the complexities associated with competing ternary phase precipitation. The interatomic spacing in pure Ag also corresponds very closely to that of pure Al, and substantial additions of silver have little effect on the lattice parameter of Al [14, 15]. Solute misfit can therefore be regarded as minimal, and solute-induced strain can be largely neglected. In addition, the chemical affinity between Ag and Cu atoms is weak and the strong co-clustering behaviour exhibited by systems such as Al-Si-Mg is not observed.

Early studies on Al-Cu-Ag alloys established that for compositions of $\sim 1\text{at.}\%(\text{Ag,Cu})$ both γ' (AlAg_2) and θ' precipitates were formed [16] and it been shown that both phases can form on dislocation loops, with θ' and γ' platelets observed at different regions of the same dislocation loop [17, 18].

We have recently shown that there is significant silver segregation around the dislocation loops at the site where θ' precipitates nucleate and that the precipitates are later surrounded by an atmosphere of silver [18]. This work examines the segregation of Ag to θ' precipitates in a Al-Cu-Ag alloy with an emphasis on the atomic structure of the Al- θ' coherent interfaces.

2 Experimental details

Alloys containing Al-0.90at.%Ag-0.90at.%Cu (Al-3.45wt.%Ag-2.05wt.%Cu) were cast from high-purity elements in air at 700°C. The composition was verified via inductively coupled plasma-mass spectroscopy (ICP-MS). The largest single impurity was Fe (0.02wt.%), with most other impurities (including Mg) present at $<0.005\text{wt.}\%$. The cast ingots were homogenised (525°C, 168 h) before being hot-rolled (to 2 mm thickness), followed by cold-rolling to 0.5 mm thickness. Further external deformation was avoided from this point onwards. Discs (3mm diameter) were punched from the sheet, solution-treated (525°C, 0.5 h) in a nitrate/nitrite salt pot and quenched to room temperature in water. Isothermal ageing of these discs was conducted in an oil bath at 200° for between 2 and 4 h.

TEM foils were prepared by manually grinding the aged discs, followed by thinning to perforation by twin jet electropolishing in a nitric acid/methanol solution ($\sim 13\text{ V}$, -20°C in 33% HNO_3 /67% CH_3OH v/v). Discs were plasma-cleaned prior to examination.

High angle annular dark field (HAADF) scanning transmission electron microscope (STEM) images were obtained using a FEI Titan³ 80-300 microscope operating at 300 kV, with convergence semi-angle of 15 mrad thus resulting in a spatial resolution of $\approx 1.2\text{ \AA}$ and with an inner collection angle of 40 mrad. By default, images are presented adjusted only for brightness and contrast. Image analysis was performed using ImageJ software, version 1.44o. EDX maps were obtained in STEM mode using a JEOL Si(Li) detector installed on a JEOL 2100F microscope operating at 200 kV with a probe size of 0.5 nm. The maps were 256x256 pixels in size, with an acquisition time of 0.2 ms per pixels over ≈ 100 frames.

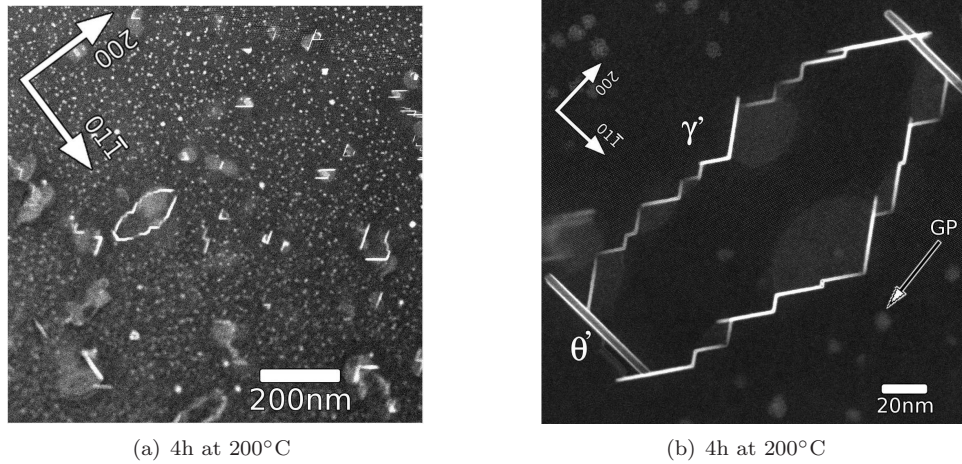


Figure 1: HAADF-STEM micrographs illustrating the microstructure of the Al-Cu-Ag alloy aged for 4 h at 200°C. (a) Low magnification image showing several precipitate assemblies (some truncated in foil preparation). (b) shows a single, similar assembly in greater detail with two θ' and a large number of γ' precipitates present. Spheroidal Ag GP zones can be seen around the assemblies in both images.

3 Results

3.1 Microstructural overview

In foils aged for 0.16–2 h at 200°C the microstructure contains only γ' (AlAg₂) precipitates and Ag-rich Guinier Preston zones (GPZ). The γ' precipitates are arranged in elliptical loops, each comprised of alternating variants, with the loop normal close to a $\langle 011 \rangle$ direction. The morphology and formation of these precipitate assemblies have been described previously [17] and are therefore not discussed in detail.

θ' precipitates are observed in samples aged for a minimum of 2 h at 200°C. Figure 1(a) presents a low magnification HAADF-STEM image obtained after 4 h ageing and shows several γ' precipitate assemblies, some of which also include θ' precipitates. Spheroidal Ag-rich GPZ are also present. Most γ' assemblies have been truncated during foil preparation; however, one complete example is present in the centre of the image.

θ' precipitates are frequently observed in pairs at opposite ends of a precipitate assembly, as is shown in Fig 1(b). Both θ' precipitates in Fig 1(b) show enhanced contrast on the coherent interfaces with the matrix, which, as will be demonstrated, is due to silver segregation.

EDX maps show segregation of silver to residual dislocations at the ends of the precipitate assemblies. Figure 2 shows HAADF-STEM images and EDX maps of θ' and γ' precipitates at the end of an assembly. Both precipitates display strong contrast in the HAADF image, as expected from the higher atomic contrast of Cu and Ag compared to Al. Between both phases a diffuse line of contrast can be seen (indicated by an arrow). EDX maps based on the Ag L peak (Fig 2(b)) show that Ag is present at the sites of both γ' and θ' phases. Ag is also concentrated along the lattice defect between γ' precipitates. The EDX map based on the Cu K peak (Fig 2(c)) shows Cu only at the site of the θ' precipitate and not at γ' or the lattice defect. Similar EDX observations of silver segregation to dislocation loops adjacent to γ' precipitate assemblies have also been reported recently [18].

These silver-enriched residual defects are also present before θ' phase precipitation. The HAADF-STEM image presented in Figure 3(a) shows two γ' precipitates with edges separated by approximately 10 nm. There is a weak diffuse line (indicated by the arrow) between the γ' precipitates indicating the presence of higher atomic number solutes. A plot of the HAADF-STEM intensity along A–A' (Fig. 3(b)) shows stronger atomic contrast in two bands, separated by approximately 1.5 nm.

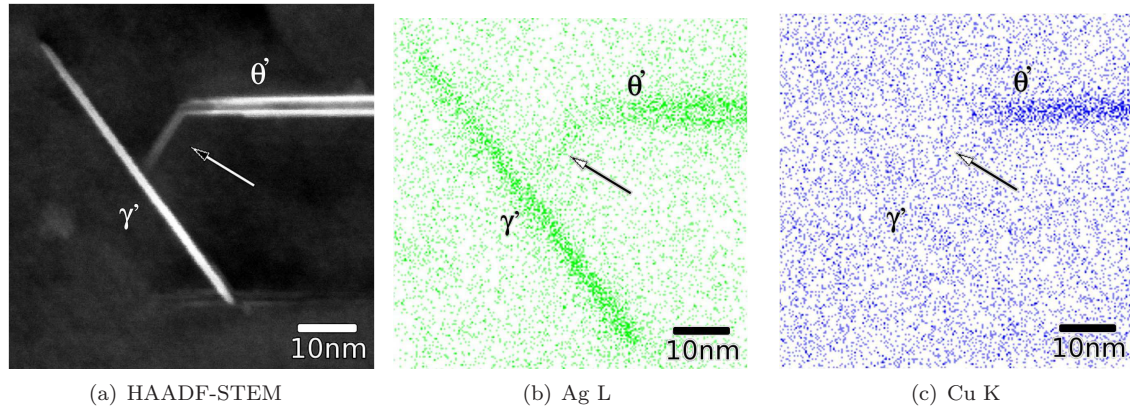


Figure 2: (a) HAADF-STEM image and (b,c) EDX maps of a γ' - θ' precipitate assembly. The Ag map (b) shows silver at the sites of both precipitates and along the defect (see arrow) between them. Cu is concentrated only at the site of the θ' precipitate.

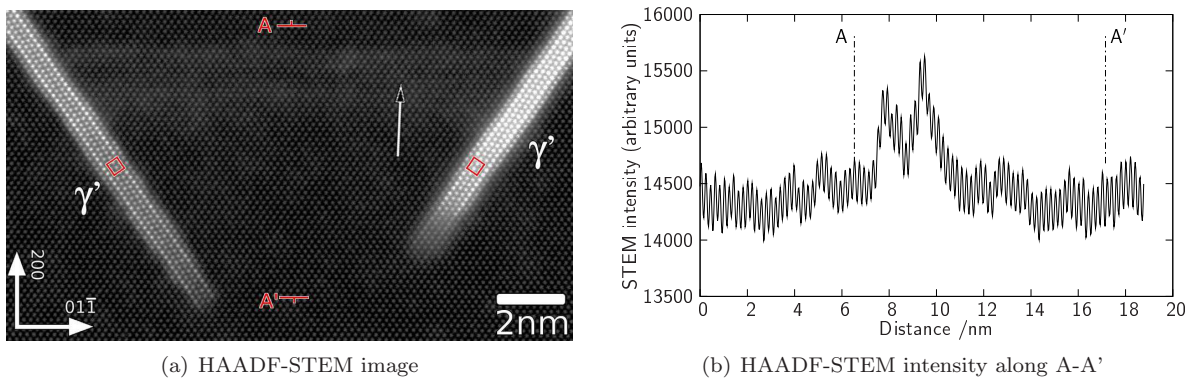


Figure 3: γ' precipitate assembly prior to θ' phase nucleation. HAADF-STEM images (a) and intensity profiles (b) show a diffuse band of higher atomic contrast elements running between the γ' precipitates. The defect (arrowed) is apparent in increased atomic contrast between the γ' precipitates. The HAADF-STEM intensity (d) indicates that the solute Ag is enriched in two bands. γ' unit cells are indicated by outlines on the micrograph.

3.2 θ' -Al interfaces

3.2.1 Coherent θ' -Al interfaces

Isothermally ageing samples for 2-4 h resulted in the precipitation of θ' platelets at the dislocation loops. Figure 4 shows representative HAADF-STEM micrographs of θ' precipitates viewed along the [011] zone axis. Figure 4(a) shows the coherent interfaces and semi-coherent edge of a θ' platelet impinging on a γ' precipitate. The coherent $(001)_{\theta'}/(001)_{Al}$ interfaces are surrounded by a bi-layer with strong atomic contrast. The HAADF-STEM intensity across the precipitate is shown in Fig 4(c). Intensity profiles have been drawn across the θ' precipitate ($A-A'$ and $B-B'$) and across the γ' phase ($C-C'$). Peaks within the θ' precipitate are due to (002) Cu layers as the atomic columns in the intervening Al (002) planes are not well resolved. Profiles A and B show a strong double-peak just outside the θ' phase (significantly greater in intensity than the Cu sites in θ') with the intensity decreasing to that of the matrix over 2-3 adjacent planes. The strong contrast in the interface layers relative to Cu sites in the θ' phase (comparable in intensity to that of the γ' precipitate) in combination with the Ag detected by EDX (Fig 2(b)) lead to the conclusion that these layers were dominated by silver ($Z=47$ vs. $Z=29$ for Cu). The layer spacing up to and including the Ag-containing bi-layer does not diverge measurably from the (200) planar spacing in the matrix.

All θ' precipitates observed in this alloy possess similar Ag-enriched coherent interfaces, although in some cases the Ag bi-layer was incomplete (e.g. Fig 4(b)). The upper face of the θ' precipitate has a uniform coverage of two strongly-contrasting atomic layers similar to that in Figure 4(a). On the bottom face this bi-layer gradually diminishes in intensity from right to left, with no clear variation in the spacing of the atomic columns. The HAADF image (Fig 4(b)) and intensity profile (Fig 4(d)) clearly show the reduction in intensity in the Ag rich layer from left ($A-A'$) to right ($C-C'$).

The atomic positions of the Ag and Cu containing layers have been verified by imaging along a second direction. Figure 5(a) shows a θ' precipitate along the [001] zone axis, with strong contrast evident in two atomic layers on both faces of the precipitate, although the upper interface is brighter than the lower. Fig 5(b) presents an example in which the Ag-rich bi-layer is absent on the upper interface and present on the lower interface, similar to Fig 4(b). In this image additional columns of Cu atoms can be seen on the outermost layer of the θ' phase (labeled “Cu(B)”), which are of comparable intensity to columns in the bulk θ' structure (“Cu(A)”). HAADF-STEM intensity profiles drawn through the θ' precipitates are shown in Fig 5(c) and 5(d). In Fig 5(c) the contrast of the lower matrix- θ' interface is weaker than that of the upper interface.

The partial Ag layers in Fig 4(b) and 5(b) allow the Cu-enriched outer layers of the θ' precipitate to be seen clearly. When viewed along the [011] direction, (Fig 4(b)) the outermost Cu layers of the θ' precipitate (labeled “Cu(B)”) have stronger contrast than Cu sites in the bulk structure (“Cu(A)”). This is evident in plots of the HAADF intensity across the precipitate (Fig 4(d)). Where the Ag layer is absent ($C-C'$ in Fig 4(b)) there is a single sharp peak corresponding to the Cu-enriched layer (labeled “Cu(B)”). The intensity of this peak is between that of the Ag enriched bi-layer and standard Cu planes of the precipitate and there is no indication of a shift in the peak position, regardless of whether Ag is present. When imaged along the [001] zone axis (Fig 4(b)) the intensity of the interface sites is consistent with the bulk sites, but, additional atomic columns (“Cu(B)”) appear between the regular (“Cu(A)”) sites. Plots of HAADF-STEM intensity (Fig. 5(d)) show a sharp single peak due to the additional Cu at the interface. These observations are consistent with a model for the introduction of additional Cu atoms at octahedral sites in θ' at the Al- θ' coherent interfaces [12]. Detailed examination reveals that similar additional Cu atomic columns are present on the opposite, Ag-rich interfaces in Fig 4(b) and 5(b) and are also present in Figures 4(a) and 5(a).

A proposed structure for the coherent interface is illustrated in Figure 6. Atomic layers are numbered for convenience, commencing from the outermost Cu-rich layer of the θ' precipitate. Cu layers labeled Cu(A) (Layers -2, -4, -6...) have the bulk structure. Those labeled Cu(B) (layer 0) have additional Cu in the octahedral interstices [12] which is responsible for stronger contrast along the [011] axis (Fig 4) and the appearance of additional atomic columns along the [001] axis (Fig. 5). Two layers outside the precipitate (labeled +2 and +3) are heavily enriched in silver, with the position of

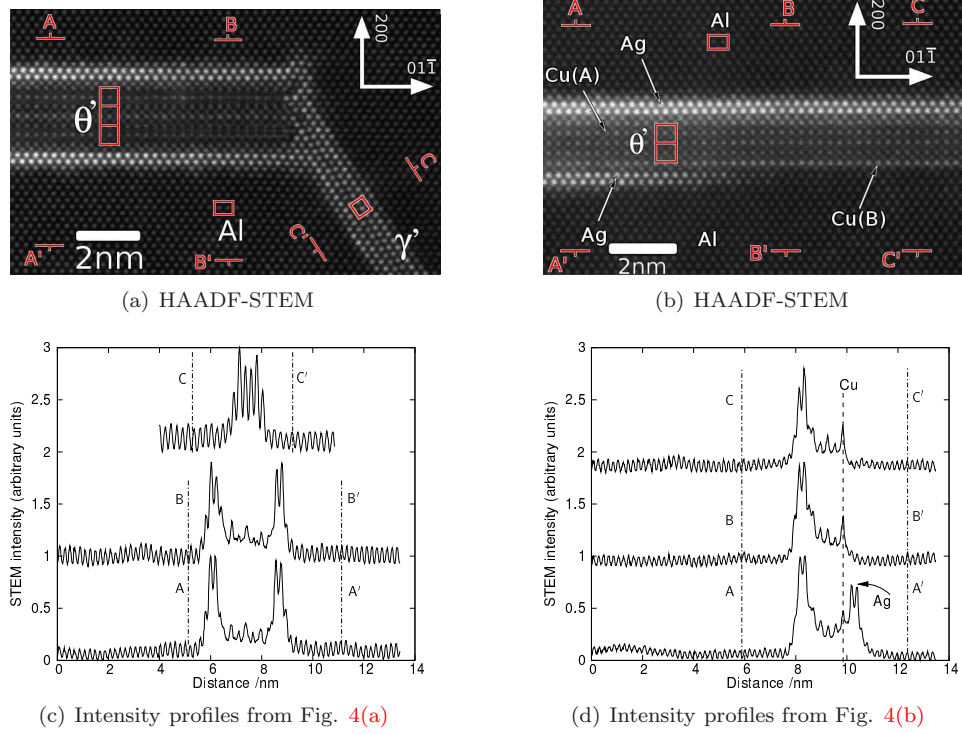


Figure 4: Ag enriched bi-layers on θ' precipitates, viewed along the $[011]$ zone axis. (a) and (b) show HAADF-STEM images of θ' precipitates with (a) complete and (b) partial Ag layers. There is a γ' precipitate adjacent to the θ' precipitate in (a). (c) and (d) show intensity profiles of HAADF-STEM image intensity across A-A', B-B', C-C' in Figures (a) and (b), respectively. Al, θ' and γ' unit cells have been outlined near the label for each phase.

the atomic columns showing no measurable deviation from the position of the matrix atom columns along both $[011]$ and $[001]$ zone axis. Although the location of these sites did not change, the HAADF-STEM intensity varies between θ' precipitates and between opposite faces and different regions of the same precipitate, suggesting a broad range of mixed Al-Ag occupancy. Atomic sites in the adjacent layer (+1) are consistent with *fcc* Al in the matrix and Al sites in the precipitate, as expected for a coherent θ' -Al interface. The atomic contrast in these columns, however, is much stronger, suggesting that this layer (and the opposite +4 layer) were partially occupied by Ag, although at a lower concentration than the +2 and +3 layer. Cu occupancy of these sites is deemed unlikely given (a) the stronger atomic contrast, (b) the shorter Cu-Al bond length compared to Al-Ag or Al-Al and (c) the unfavourable Cu-Ag bond enthalpy, and (d) recently published EDX maps showing no detectable Cu surrounding the precipitate [18].

3.2.2 Semi-coherent θ' -Al interfaces

The semi-coherent θ' -Al interfaces are frequently enriched in silver. Of a total of 40 instances in which the semi-coherent interface are clearly resolved, in 16 cases (40%), the interfaces are completely covered by a double layer of silver. In the remainder of the precipitates the Ag-rich bi-layer is either absent or incomplete. Figure 7 shows representative examples of semi-coherent edges of θ' precipitates with Ag bi-layers along (a) $[011]$ and (b) $[001]$ zone axes. In Fig. 7(a) the precipitate directly impinges on a γ' precipitate. The semi-coherent interface is decorated with a bi-layer of Ag, similar to that present on the coherent interfaces. The edge of the θ' precipitate is jagged, with the adhering Ag bi-layer having facets that alternate between $(1\bar{1}1)$ and $(\bar{1}\bar{1}1)$ planes. It is notable that these are preferred habit planes

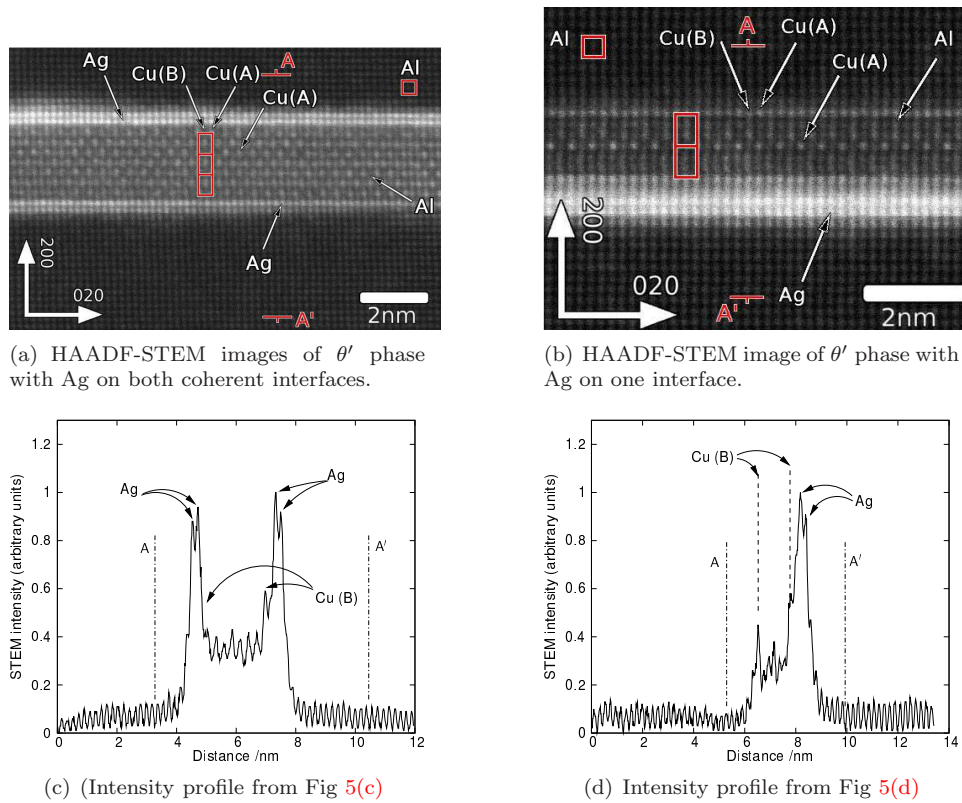


Figure 5: Ag enriched bi-layers on θ' precipitates, viewed along the [001] zone axis. (a) and (B) show HAADF-STEM images of θ' precipitates with (a) near complete and (b) partial Ag bi-layers. There is a γ' precipitate adjacent to the θ' precipitate in (a). (c) and (d) show intensity profiles of HAADF-STEM intensity across the precipitates in Figures (a) and (b), respectively. In (b) and (d) the stronger contrast in the outer layers of the θ' structure (labeled Cu(B)) can be seen. θ' unit cells have been indicated by outlines.

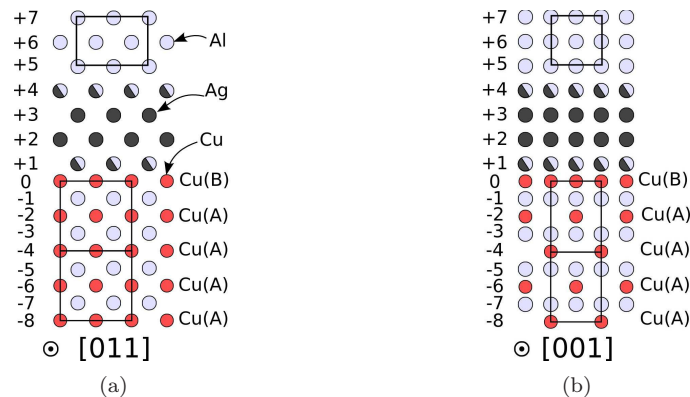


Figure 6: A structural model for the coherent θ' -matrix interface in an Al-Cu-Ag alloy. Ag is concentrated into two layers, separated from θ' by a single layer of mixed Al/Ag. Cu layers with the bulk structure are designated Cu(A), while the interface layers with additional Cu in octahedral interstices are designated Cu(B). The solid outlines indicate Al and θ' unit cells.

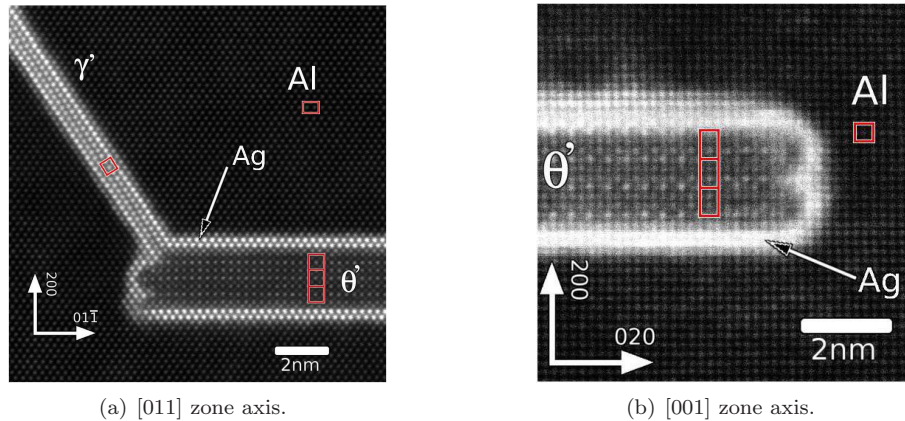


Figure 7: Ag segregation to semi-coherent θ' -Al interfaces. Foils were aged for 4h at 200°C. Ag is concentrated in two atomic layers adjacent to the semi-coherent interface and in (a) shows facets parallel to $\{111\}$ planes. Al, θ' and γ' unit cells have been outlined.

for the γ' (AlAg_2) phase, having the lowest interfacial energy [19]. The semi-coherent interfaces are less well resolved along the $[001]$ zone, (Fig. 7(b)); however, the Ag layer can still be seen to be two atomic layers in thickness.

4 Discussion

4.1 θ' phase precipitation in Al-Cu-Ag alloys

Precipitation of the θ' phase in Al-0.90at.%Cu-0.90at.%Ag alloys is observed on pre-existing assemblies of γ' precipitates. Precipitation in the form of extended arrays or on dislocations is not observed in this alloy, indicating either that the dislocation loops offer a more favourable nucleation site, or that the extended array morphology is prevented from forming. Recently reported diffraction contrast images of the γ' precipitate assembly obtained before the nucleation of θ' precipitates show diffuse, linear contrast features lying along $[1\bar{1}0]$ directions at either end of the assemblies [18]. These have been shown to be segments of dislocation loops tangential to the (100) planes and dark-field imaging was used to show that the dislocation loop segment had dissociated [18] as reported for precipitation of the θ' phase colonies on dislocations [20] to yield a body-centred tetragonal stacking fault between partial dislocations with Burgers vectors of type $1/2\langle 001 \rangle$. Here it is shown using HAADF-STEM imaging and EDX mapping (Fig 3) that Ag segregates to these defects, whereas the level of Cu was not measurably enhanced. Given that the dislocation is dissociated at this stage, despite the absence of Cu, it is evident that Ag segregation is responsible for the dislocation splitting. While there are no reports of Ag promoting dissociation of a dislocation in this way it has been established that the stacking fault energy of Al close-packed (111) planes decreases locally for high levels of silver [21].

4.2 Silver segregation to θ' -Al interfaces

Interfacial energy, rather than strain, is the most probable cause for the formation of the Ag-rich bi-layers. The Al-Al, Ag-Ag bond lengths are 286.3 pm and 288.9 pm, respectively, and substitution of Ag for Al is not expected to relieve volumetric strain associated with the precipitate. In addition, measurable atomic displacements in atomic planes outside the θ' structure are not seen in plots of the peak position (Fig 4(d), 5(d)), suggesting that the θ' structure is not disrupted by the presence of the Ag bi-layer.

Table 1: Bond enthalpies (kJ/mol) for gaseous diatomic species [24].

	Al	Ag	Cu
Al	133±5.8	183.7±9.2	227.1±1.2
Ag		159±2.9	171.5±9.6
Cu			201

The generation of the Ag-rich bi-layer involves the loss of θ' -Al and γ' -Al interfaces (as γ' precipitates are removed) and the formation of a Al-Ag-Al-Cu interface. Calculations of the interface energies for the Al- θ' coherent precipitate-matrix interfaces have provided values¹ ranging from 156 mJ.m⁻² using molecular dynamics [22] to 190 mJ.m⁻² for some first-principles calculations [23]. Discrete lattice plane method calculations for coherent γ' -Al {111} interfaces estimated a much lower energy of 6.5 mJ.m⁻², with facets on other planes in the range 6.3-7.1 mJ.m⁻² [19]. Wetting of the {001} θ' -Al coherent interface would therefore reduce the interfacial energy with the matrix by replacing the higher energy θ' -Al interface with a Ag-Al interface.

The existence of a single atomic layer between a precipitate and the surrounding Ag interface layers was also observed for Ω precipitates in Al-Cu-Mg-Ag alloys [9]. According to density functional theory calculations [10], Mg occupancy of this layer gave the lowest energy structure; however, it was reported that there was no clear indication of additional Mg in or around the precipitates [9], which would infer that this layer contains Al. In the present alloy, Mg is a trace-level impurity and this layer undoubtedly consists principally of Al, with the stronger atomic contrast (See Fig 4,5) suggesting partial Ag occupancy.

The presence of Al atoms in this layer is probably due to the relative bond enthalpies². Although atomistic calculations such as by density functional theory are required to confirm this view, the following explanation appears plausible. In the absence of this layer, the Cu-terminated θ' interface would be in contact with Ag (bond enthalpy for (171.5±9.6 kJmol⁻¹). With this layer in place the system is able to form stronger Al-Cu (227.1±1.2 kJmol⁻¹) and Al-Ag (183.7±9.2 kJmol⁻¹) bonds (see Table 1).

There appears to be no structural or chemical alteration in the θ' phase, despite the presence of the Ag bi-layer. The outermost layer of the θ' phase even contains additional Cu atoms in octahedral sites, as has recently been demonstrated in binary Al-Cu [12]. This points to an interaction in which Ag chemically wets the Al- θ' interface, given sufficient solute supply, lowering the interfacial energy, without substantially affecting the θ' phase.

A substantial amount of Ag is required to form a interface bi-layer and larger θ' precipitates with partial Ag coverage are observed (e.g. Figs 5(a) and 5(b)), suggesting that the Ag supply can become deficient. In an earlier study on Al-Cu-Ag aged for 16–72 h [25] the γ' assemblies were rarely seen. The most prominent feature were paired θ' precipitates, separated by roughly the same spacing as the width of the γ' assemblies with few remaining γ' precipitates. It therefore appears likely that silver is drawn not only from solution and GP zones, but from the neighbouring γ' precipitates, leading to the disruption and eventually consumption of the precipitate assembly. This in itself suggests a strong chemical interaction for the interface Ag to be preferred over the γ' structure.

Some 40% of semi-coherent θ' interfaces are completely covered with Ag. The Ag bi-layer followed the shape of the precipitate edge closely, with a tendency for faceting along {111} planes. Discrete lattice plane calculations show that the {111}_{Al}/(0001) _{γ'} interface had an extremely low chemical interfacial energy of 5-7 mJ.m⁻² [19]. The presence of such a silver bi-layer seems to preclude further lengthening of the θ' precipitate, since Cu solute would have to diffuse through 2 atomic layers of silver, with which it has a weaker bond enthalpy than with Al (227.1 *vs.* 171.5 kJmol⁻¹).

¹These calculations were based on the bulk structure, and did not include the addition Cu sites at the interface [12]. It is unlikely, however that this would substantially affect the interfacial energy.

²Bond enthalpies are given as the values for gaseous diatomic species to provide a qualitative comparison of the relative bonding strength.

It is unclear whether the Ag-enriched bi-layer affects the preferred thicknesses [26] or thickening behaviour of the θ' phase. An investigation into the thickening behaviour of θ' precipitates in Al-Cu-Ag is underway.

4.3 Comparison with other Al alloy systems

This study highlights that the details of the precipitate-matrix interface are strongly system dependent and that the matrix or precipitate may undergo compositional and structural changes. In Al-Cu binary alloys, it is the structure of the θ' precipitate that differs from that of the bulk phase, with additional Cu atoms present at the interface [12]. Silicon additions to Al-Cu alloys also affect the precipitate composition. Atom-probe measurements found a factor of >11 increase in the Si content at the coherent θ' -Al interface in Al-4at.%Cu-0.02at.%Si alloys, which density functional theory calculations attributed to Si substituting for Cu in the precipitate [11].

In alloys containing Ω phase precipitates, it is the matrix composition that changes, with the formation of a Ag/Mg interface bi-layer [7, 8, 9]. The Ag-enriched bi-layers shown here in Al-Cu-Ag alloys bear striking similarities to the Mg/Ag bi-layers surrounding Ω phase precipitates. However, there was no evidence of an interface layer on the semi-coherent edges of Ω precipitates (see, for example Fig. 5 and 8 in [9]), whereas such layers is frequently observed on θ' precipitates (e.g. Figs 4(a) and 7). It should also be noted that density functional theory calculations predict that only a combination of Mg and Ag stabilises the Ω -Al interface and that charge transfer from Mg may play a role in this effect [10]. In this study, Mg was present only as an impurity element at levels of <0.005wt.% (\approx 0.005at.%, compared to 0.90at.%Ag) and it appears very unlikely that Mg plays any role in the bi-layers in Al-Cu-Ag alloys.

The observation of additional Cu in the outermost layer of the θ' phase shows that this phenomenon is not unique to θ' precipitates in binary Al-Cu and can exist despite the presence of a Ag interface bi-layer. In Al-Cu-Ag alloys, therefore, both the matrix and precipitate undergo changes at the interface. This highlights the complexity of interface interactions and the possibility for compositional or structural deviations in the matrix (Ag bi-layers in Al-Cu-Ag, Ag/Mg bi-layers in Al-Cu-Mg-Ag) and/or precipitate (extra Cu in θ' in Al-Cu and Al-Cu-Ag, Ω precipitation in Al-Cu-Mg-Ag, Si substitution in θ' Al-Cu-Si).

Finally, it should be noted that the appearance of the thin γ' precipitates was also of interest. Single unit cell thickness γ' precipitates (Fig. 3(a), 4(c) and 7(a)) did not show the alternating strong and weak contrast that was expected for the Ag-rich and Al-rich layers in this structure [27, 28]. In an earlier report on thickening of γ' precipitates, we noted that Ag and Al did not appear to be ordered in single unit cell thickness γ' precipitates [29] and an investigation into ordering of silver in γ' precipitates in Al-Cu-Ag alloys is underway.

5 Conclusions

θ' (Al_2Cu) precipitates in Al-Cu-Ag alloys were examined using EDX mapping and high resolution HAADF-STEM imaging. Silver (Ag) played several roles in the nucleation and growth of θ' precipitates on dissociated segments of dislocation loops.

1. Ag in solid solution facilitates dissociation of the dislocation loop to provide an isostructural surface between $1/2\langle 100 \rangle$ -type partial dislocations, assisting in the nucleation of the θ' phase.
2. Ag segregates to the coherent interfaces of the θ' precipitates, forming an Ag-rich bi-layer. This bi-layer is thought to reduce the chemical component of the interfacial energy between θ' and the matrix. As θ' precipitates lengthen, Ag is drawn from the adjacent regions and neighbouring γ' (AlAg_2) precipitates, leading to the gradual shrinkage and loss of the γ' precipitates.

3. Ag also segregated to approximately 40% of the semi-coherent θ' -matrix interfaces, where it appears to act as a barrier to Cu diffusion, thus impeding or preventing lateral growth of the θ' precipitates.

Acknowledgments

The authors gratefully acknowledge the support of the Australian Research Council through the Centre of Excellence for Design in Light Metals. The experiments were conducted at the Monash Centre for Electron Microscopy and we acknowledge the use of the facilities and engineering support by Russell King. We also thank Dr. Brian Pauw for valuable comments on the manuscript. Finally we are thankful for the support and encouragement of Professor Barrington C. Muddle, whose work initiated this project.

References

- [1] A. Wilm. *Metallurgie*, 8:225, 1911.
- [2] F.W. Gayle and M. Goodway. Precipitation hardening in the first aerospace aluminum-alloy—the Wright flyer crankcase. *Science*, 266(5187):1015–1017, 1994. doi: [10.1126/science.266.5187.1015](https://doi.org/10.1126/science.266.5187.1015)
- [3] A. W. Zhu, B. M. Gable, G. J. Shiflet, and E. A. Starke, Jr. The intelligent design of age hardenable wrought aluminum alloys. *Adv. Eng. Mater.*, 4(11):839–846, 2002. doi: [10.1002/1527-2648\(20021105\)4:11<839::AID-ADEM839>3.0.CO;2-8](https://doi.org/10.1002/1527-2648(20021105)4:11<839::AID-ADEM839>3.0.CO;2-8).
- [4] L. Bourgeois, C. Dwyer, M. Weyland, J.-F. Nie, and B. C. Muddle. The magic thicknesses of θ' precipitates in Sn-microalloyed Al-Cu. *Acta Mater.*, 2011. doi: [10.1016/j.actamat.2011.10.015](https://doi.org/10.1016/j.actamat.2011.10.015).
- [5] J. M. Silcock. Intermediate precipitates in aged binary alloys of aluminium with cadmium, indium or tin. *J. Inst. Metal*, 84:19–22, 1955.
- [6] J. M. Silcock. The structural ageing characteristics of ternary aluminium-copper alloys with cadmium, indium or tin. *J. Inst. Metal*, 84:23–35, 1955.
- [7] E. Okunishi, K. Ibe, and K. Hono. High-resolution nano area analysis of plate like precipitate in aluminum alloy employed with Z-contrast and drift corrected EDS mapping. *J Japan Inst Metal*, 65(5):419–422, 2001.
- [8] K. Hono, N. Sano, S. S. Babu, R. Okano, and T. Sakurai. Atom probe study of the precipitation process in Al-Cu-Mg-Ag alloys. *Acta Metall. Mater.*, 41(3):829–838, 1993.
- [9] C. R. Hutchinson, X. Fan, S. J. Pennycook, and G. J. Shiflet. On the origin of the high coarsening resistance of Ω plates in Al-Cu-Mg-Ag alloys. *Acta Mater.*, 49:2827–2841, 2001.
- [10] Lipeng Sun, Douglas L. Irving, Mohammed A. Zikry, and D. W. Brenner. First-principles investigation of the structure and synergistic chemical bonding of Ag and Mg at the Al | Ω interface in a Al-Cu-Mg-Ag alloy. *Acta Mater.*, 57(12):3522–3528, 2009. doi: [10.1016/j.actamat.2009.04.006](https://doi.org/10.1016/j.actamat.2009.04.006).
- [11] A. Biswas, D. J. Siegel, C. Wolverton, and D. N. Seidman. Precipitates in Al-Cu alloys revisited: Atom-probe tomographic experiments and first-principles calculations of compositional evolution and interfacial segregation. *Acta Mater.*, 59(15):6187–6204, 2011. doi: [10.1016/j.actamat.2011.06.036](https://doi.org/10.1016/j.actamat.2011.06.036).
- [12] L. Bourgeois, C. Dwyer, M. Weyland, J.-F. Nie, and B. C. Muddle. Structure and energetics of the coherent interface between the θ' precipitate phase and aluminium in Al-Cu. *Acta Mater.*, 59:7043–7050, 2011. doi: [10.1016/j.actamat.2011.07.059](https://doi.org/10.1016/j.actamat.2011.07.059).

- [13] S. Liu, S. Zhao, and Q. Zhang. Phase diagram of the aluminium-copper-silver alloy system. *Acta Metall. Sinica*, 19:70–73, 1983.
- [14] W. Hume-Rothery and G. V. Raynor. The apparent sizes of atoms in metallic crystals with special reference to aluminium and the electronic state of magnesium. *Philos. Trans. R. Soc. London, Ser. A*, 177(968):27–37, 1940.
- [15] L. Vegard. Die konstitution der mischkristalle und die raumfüllung der atome. *Z. Metallkd.*, 5:2–11, 1921.
- [16] G. Bouvy and R. Graf. Etude du durcissement et de la structure de trois alliages ternaires Al-Cu-Ag derives de l'alliage binaire Al-Cu 4 percent. *C. R. Acad. Sci.*, 260(18):4742–4845, 1965.
- [17] J. M. Rosalie, L. Bourgeois, and B. C. Muddle. Precipitate assemblies formed on dislocation loops in aluminium-silver-copper alloys. *Philos. Mag.*, 89(25):2195–2211, 2009. doi: [10.1080/14786430903066959](https://doi.org/10.1080/14786430903066959).
- [18] J. M. Rosalie, L. Bourgeois, and B. C. Muddle. Precipitation of the θ' (Al_2Cu) phase in Al-Cu-Ag alloys. In *Light alloys*, volume 141, pages 307–312. TMS (The Minerals, Metals and Materials Society), 2012.
- [19] R. V. Ranamujan, J. K. Lee, and H. I. Aaronson. A discrete lattice plane analysis of the interfacial energy of coherent F.C.C:H.C.P. interfaces and its application to the nucleation of γ in Al-Ag alloys. *Acta Metall. Mater.*, 40(12):3421–3432, 1992.
- [20] U. Dahmen and K. H. Westmacott. The mechanism of θ' precipitation on climbing dislocations in Al-Cu. *Scr. Metall.*, 17(10):1241, 1983. doi: [10.1016/0036-9748\(83\)90292-2](https://doi.org/10.1016/0036-9748(83)90292-2).
- [21] T. C. Schulthess, P. E. A. Turchi, A. Gonis, and T. G. Nieh. Systematic study of stacking fault energies of random Al-based alloys. *Acta Mater.*, 46:2215–2221, 1998.
- [22] S. Y. Hu, M. I. Baskes, M. Stan, and L. Q. Chen. Atomistic calculations of interfacial energies, nucleus shape and size of θ' precipitates in Al-Cu alloys. *Acta Mater.*, 54(18):4699–4707, 2006.
- [23] V. Vaithyanathan, C. Wolverton, and L. Q. Chen. Multiscale modeling of θ' precipitation in Al-Cu binary alloys. *Acta Mater.*, 52(10):2973–2987, 2004. doi: [10.1016/j.actamat.2004.03.001](https://doi.org/10.1016/j.actamat.2004.03.001).
- [24] Y. R. Lup and J. A. Kerr, editors. *CRC handbook of chemistry and physics*, chapter “Bond dissociation energies”. Number 86. Taylor and Francis, 2005.
- [25] J. M. Rosalie, L. Bourgeois, and B. C. Muddle. Nucleation of intermediate phases in aluminium-silver-copper alloys. In *Solid-Solid Phase Transformations in Inorganic Materials*, volume 1; Diffusional transformations, pages 41–46. TMS, 2005.
- [26] W. M. Stobbs and G. R. Purdy. Elastic accommodation of semi-coherent θ' in Al-4 wt-percent Cu alloy. *Acta Metall.*, 26(7):1069–1081, 1978. doi: [10.1016/0001-6160\(78\)90135-9](https://doi.org/10.1016/0001-6160(78)90135-9).
- [27] J. M. Howe. High-resolution tem of precipitates and interfaces. *J. Metal*, pages 13–16, 1987.
- [28] N. A. Zarkevich, D. D. Johnson, and A. V. Smirnov. Structure and stability of hcp bulk and nano-precipitated Ag_2Al . *Acta Mater.*, 50:2443–2459, 2002.
- [29] J. M. Rosalie, L. Bourgeois, and B. C. Muddle. Nucleation and growth of the γ' (AlAg_2) precipitate in Al-Ag(-Cu) alloys. *Acta Mater.*, 59(19):7168–7176, 2011. doi: [10.1016/j.actamat.2011.08.001](https://doi.org/10.1016/j.actamat.2011.08.001).